

Barbie: Text to Barbie-Style 3D Avatars

Xiaokun Sun¹, Zhenyu Zhang^{1*}, Ying Tai¹, Qian Wang², Hao Tang³, Zili Yi¹, Jian Yang¹

¹Nanjing University ²China Mobile Research Institute ³Peking University

xiaokun_sun@smail.nju.edu.cn, zhangjesse@foxmail.com, {yingtai, yi, csjyang}@nju.edu.cn,
wangqianrg@chinamobile.com, bjdxtanghao@gmail.com

<https://xiaokunsun.github.io/Barbie.github.io>



Figure 1. Using only texts as input, our method can generate Barbie-style 3D avatars. “Barbie-style” refers to: (1) high-quality and diverse generated 3D avatars; (2) disentangled generation of the body, garments, and accessories; and (3) support for seamless apparel composition, editing, and user-friendly animation, **similar to Barbie dolls**.

Abstract

Recent advances in text-guided 3D avatar generation have made substantial progress by distilling knowledge from diffusion models. Despite the plausible generated appearance, existing methods cannot achieve fine-grained disentanglement or high-fidelity modeling between inner body and outfit. In this paper, we propose Barbie, a novel framework for generating 3D avatars that can be dressed in diverse and high-quality Barbie-like garments and accessories. Instead of relying on a holistic model, Barbie achieves fine-grained disentanglement on avatars by semantic-aligned separated models for human body and outfits. These disentangled 3D representations are then optimized by specialized expert models to guarantee the domain-specific fidelity. To balance geometry diversity and reasonableness, we propose a series of losses for template-preserving and human-prior evolving. The final avatar is

enhanced by unified texture refinement for superior texture consistency. Extensive experiments demonstrate that Barbie outperforms existing methods in both dressed human and outfit generation, supporting flexible apparel combination, editing, and animation.

1. Introduction

In recent years, the creation of 3D digital humans has garnered significant attention due to its widespread applications in AR/VR. These applications yield the generated 3D avatars to have exquisite geometry, lifelike appearance, ultra-high diversity, and a faithful disentanglement of the human body and apparel. Usually, manually sculpting holistic 3D virtual humans is highly labor-intensive and time-consuming. Although progress [5, 48, 61] has been made on learning-based automatic human generation, these methods require large amounts of 3D human data for training, which greatly limits their application scope.



Figure 2. Compared to holistic methods, Barbie effectively decouples the human body from different apparels while exhibiting fine details in the hands and head. In contrast to disentangled approaches, Barbie demonstrates a notable quality advantage and is capable of generating detailed accessories.

With recent advancements in text-to-image [65] and text-to-3D [58] models, leveraging natural language inputs for avatar generation has become increasingly popular.

The aforementioned text-to-avatar works can be roughly divided into two categories: generating (1) a holistic avatar and (2) disentangled models on body and apparel. Works on the former one [23, 32, 42] are based on text-to-3D generation frameworks [4, 43, 58], and combined with human prior knowledge [1, 46, 57] to improve the geometry fidelity of the generated results. However, these works treat the human body, clothes, and accessories as a holistic model, which results in a loss of flexibility on applications such as virtual try-on and garment transfer. As illustrated in Fig. 2-(a), these works cannot properly control garments and accessories with prompt. Consequently, a series of disentangled text-to-avatar works [14, 25, 72] have emerged. These methods employ multi-stage optimization strategies to model the body and clothes separately. However, these methods adopt a single general diffusion model to guide both body and garment generation, resulting in domain-specific fidelity loss on geometry or texture details. Furthermore, as illustrated in Fig. 2-(b), they fail to generate diverse and realistic outfits such as necklaces, glasses, hats, watches, or other accessories. The reason behind is two-fold: these methods lack of (1) fine-grained decomposition on avatar representation; (2) suitable constraints for optimization to generate in-domain components. In addition to this, generating fine-grained disentangled 3D avatars with realistic and text-aligned bodies, as well as garments and accessories, is still an open problem.

In this paper, we propose **Barbie**, a novel framework for generating Barbie-style 3D avatars that can be dressed in high-fidelity and diverse outfits, similar to the design of Barbie dolls. As shown in Fig. 1, the avatars generated by Barbie have exquisite geometry and textures, and meanwhile wear various generated high-quality clothes and accessories that can be freely combined and edited. Instead of generating bodies and all kinds of outfits guided by a single text-to-image (T2I) model, Barbie suitably involves different expert diffusion models to guarantee the domain-specific fidelity. Concretely, we first initialize different components of an avatar with semantic-aligned human prior to get disentangled representations. Then, each representation is op-

timized by corresponding expert T2I models to generate in-domain geometry and texture. During optimization, we propose SMPLX-evolving prior loss to enhance the diversity and description alignment for body generation, and a template-preserving loss to suppress the artifacts of generated outfits. Finally, to balance the effect of different expert models, we propose an unified texture refinement to jointly optimize the composed avatar for more realistic appearance generation. In this way, the generated 3D avatars are disentangled and interactive with high-fidelity body, garments, and accessories, which is actually "**Barbie-style**".

Our main contributions are summarized as follows:

- We propose Barbie, a novel framework for creating realistic and highly disentangled 3D avatars in diverse body, garments, and accessories. To the best of our knowledge, Barbie should be the first work that achieves fine-grained text-to-avatar generation.
- We effectively employ expert models at different optimization stages to provide suitable guidance, boosting the generation quality on domain-specific realism. A series of novel losses and strategies are also proposed to address the geometry and texture conflicts when combining different expert models.
- Extensive experiments demonstrate that Barbie outperforms existing methods on avatar/outfit generation, showing superior geometry, texture, alignment on text description, and ability on fine-grained disentanglement.

2. Related Work

Text to 3D Content Generation. Motivated by text-guided image generation, many works have focused on zero-shot 3D content generation from text prompts. Early methods [28, 52, 66] use the CLIP model [60] to align 3D representations with text descriptions, but the quality is unsatisfactory. DreamFusion [58] introduces a score distillation sampling (SDS) loss, enabling higher-fidelity 3D content by leveraging a stronger pre-trained T2I model [65]. Later works improve text-to-3D generation through advancements in 3D representations [4, 77], optimization strategies [43, 70], SDS loss [41, 75], and diffusion models [40, 59, 69]. However, these methods do not fully utilize the rich prior of the human body or generate realistic and high-quality 3D avatars.

Text to Holistic 3D Avatar Generation. AvatarCLIP [23] first realizes the zero-shot generation of 3D digital humans from text prompts by integrating human prior knowledge into Neus [73]. With the introduction of SDS loss [58], many subsequent works [3, 29, 32, 50] combine it with parametric human models [1, 46, 57], significantly improving the fidelity of the generated 3D digital humans. In addition, AvatarVerse [79] and DreamWaltz [27], inspired by ControlNet [80], greatly enhance the 3D consistency of the generated results by adopting conditional diffusion mod-

els. TADA [42] and X-Oscar [49] propose using a subdivided SMPL-X model [57] instead of implicit NeRF [51] and Neus [73] to represent 3D digital humans. HumanNorm [26] and SeeAvatar [76] achieve impressive geometric details by combining DMTet [68] with decoupled optimization strategies. Recently, HumanGaussian [44] and GAvatar [78] introduced 3D Gaussian Splatting [31] to create fast-rendering high-quality 3D avatars. However, these approaches typically treat the human body, garments, and accessories as a holistic model, which loses the flexibility and controllability of generation for further applications, such as the composition and editing of clothing.

Text to Disentangled 3D Avatar Generation. To realize controllable avatar generation, a series of decoupled approaches have been proposed that separately model the human body and clothing through multi-stage optimization. Humancoser [74] and AvatarFusion [25] using two radiation fields [51, 73] to represent the human body and all clothes, respectively. LAGA [16] and TELA [14] employ a layer-wise framework, representing each piece of clothing as an independent layer, further enhancing the flexibility and controllability of the generation. SO-SMPL [72] replaces implicit representations [51, 73] with a more explicit SMPL-X [57] representation. However, these works employ a single general T2I model to guide both body and clothing generation, leading to a loss of geometry or texture fidelity in specific domains. Furthermore, they are unable to generate diverse and realistic outfits, such as necklaces, glasses, hats, watches, or other accessories.

In contrast to previous methods, the digital human generated by Barbie not only has fine geometry and realistic appearance, but also wears multiple separable high-quality clothes and accessories. We summarize the main differences between Barbie and related approaches in Fig. 2.

3. The Proposed Method

3.1. Preliminaries

SMPL-X [57] is a parametric human model that represents the full-body shape, pose, and expression using a small number of parameters. Given a set of shape parameters β , body pose parameters θ_{body} , jaw pose parameters θ_{face} , finger pose parameters θ_{hand} , and expression parameters ψ_{exp} , it can generate a 3D human mesh M .

Score Distillation Sampling [58] leverages a pre-trained T2I model to guide the 3D representation to align with the input text. Given a text prompt y , a 3D representation with parameters θ , and a diffusion model with parameters ϕ , the SDS loss is defined as follows:

$$\nabla_{\theta} \mathcal{L}_{SDS} = \mathbb{E}_{t, \epsilon} \left[w(t) (\epsilon_{\phi}(x_t; y, t) - \epsilon) \frac{\partial x}{\partial \theta} \right], \quad (1)$$

where t is the time step in the 2D diffusion model, $x = g(\theta)$ is the image rendered from θ by a differentiable renderer g ,

$x_t = x + \epsilon$ is a noised version of x , $\epsilon_{\phi}(x_t; y, t)$ is the denoised image, and $w(t)$ is the weight function. For simplicity, we omit $w(t)$ in the following formulas.

DMTet [68] is a hybrid representation consisting of an implicit signed distance function (SDF) and a differentiable Marching Tetrahedral layer for transferring implicit SDF to an explicit mesh. The SDF can be efficiently represented by an MLP with multi-resolution hash encoding [53].

3.2. Overview

Given a prompt, Barbie aims to generate a disentangled 3D avatar dressed in high-fidelity and diverse garments and accessories, similar to Barbie dolls. Fig. 3 shows the overview of the pipeline with three crucial stages. To guarantee the quality of generated body and outfits, we employ targeted expert diffusion models with specific regularization to produce a high-fidelity and reasonable human body (Sec. 3.3) and outfits (Sec. 3.4). The final composed avatar is jointly fine-tuned with unified texture refinement to achieve a more harmonious and consistent appearance (Sec. 3.5).

3.3. Human Body Generation

Human Body Initialization. Following HumanNorm and RichDreamer, we adopt DMTet as our 3D representation. Since DMTet is highly sensitive to initialization, we use SMPL-X mesh to build an accurate initial input. Concretely, we employ a differentiable renderer [33] and SDS loss to optimize the shape parameters β according to the input base human body description, thereby determining the basic body shape of the digital human. This initialized SMPL-X mesh M_{init} will be used in subsequent stages to provide rich human prior knowledge and ensure a semantic-aligned representation for the outfit.

Human Body Geometry Modeling. We then learn to optimize the initialized DMTet into disentangled geometry and texture. As discussed in introduction, using a single general T2I model struggles to provide domain-specific constraints to create realistic human body or outfits. Therefore, we employ human-specific diffusion models in HumanNorm [26] which is fine-tuned with high-fidelity 3D human data for detailed body modeling.

In particular, human-specific diffusion models include a normal-adapted diffusion model ϕ_{hn} , a depth-adapted diffusion model ϕ_{hd} , as well as a normal-conditioned diffusion model ϕ_{hc} for human texture creation. ϕ_{hn} and ϕ_{hd} fully capture human geometry information and generate high-quality normal and depth images based on the input minimal-clothed human body description y_{h} . These models optimize the initialized human DMTet parameterized by θ_{h} with the following SDS loss:

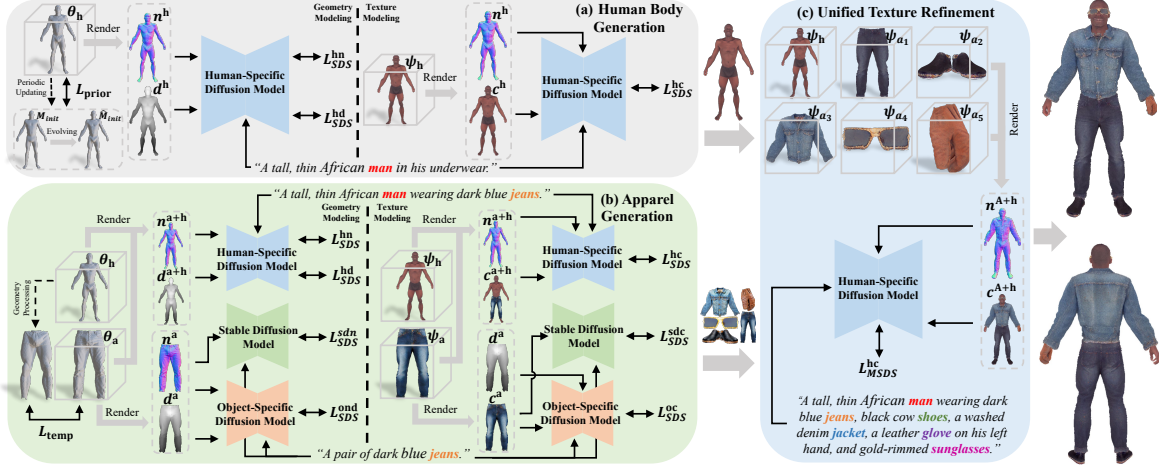


Figure 3. Barbie consists of three stages: (a) Using human-specific diffusion models and SMPLX-evolving prior loss, Barbie generates a plausible and high-fidelity basic human body; (b) Initializing with the semantic-aligned template mesh, Barbie creates high-quality clothes and accessories piece by piece using object-specific diffusion models and template-preserving loss; (c) Finally, Barbie jointly fine-tunes the assembled avatar to further enhance the texture harmony and consistency.

$$\nabla_{\theta_h} \mathcal{L}_{SDS}^{hn} = \mathbb{E}_{t,\epsilon} \left[(\epsilon_{\phi_{hn}}(n_t^h; y_h, t) - \epsilon) \frac{\partial n^h}{\partial \theta_h} \right], \quad (2)$$

$$\nabla_{\theta_h} \mathcal{L}_{SDS}^{hd} = \mathbb{E}_{t,\epsilon} \left[(\epsilon_{\phi_{hd}}(d_t^h; y_h, t) - \epsilon) \frac{\partial d^h}{\partial \theta_h} \right], \quad (3)$$

where n^h and d^h are the rendered normal and depth maps of the human body, respectively.

SMPLX-Evolving Prior Loss. Although Eq. (2) and Eq. (3) leads to detailed human body generation, the overly strong generative prior of human-specific diffusion models may urge the generated results to overfit the input text, resulting in unnatural geometry and exaggerated body proportions (see Sec. 4.4). A straightforward approach is to introduce parametric human body models (e.g. SMPL-X) and provide human body priors using the following equation:

$$\mathcal{L}_{\text{prior}} = \sum_{p \in P} \|s_{\theta_h}(p) - s_{\text{init}}(p)\|_2^2, \quad (4)$$

where s_{θ_h} and s_{init} represent the SDF functions of the generated body DMTet and the initialized SMPL-X mesh M_{init} , respectively, and P is a set of randomly sampled points in space. However, due to the overly smooth geometry of SMPL-X, this approach may lead to a reduction in diversity and rich detail. Another potential solution is the evolving constraint proposed by SeeAvatar [76] to periodically improve the initial DMTet template. Although producing reasonable geometry, this approach discards the original topology and semantics of SMPL-X, and thus becomes unfriendly to garment initialization or avatar animation.

To address this problem, we propose an SMPLX-evolving prior loss that evolves the SMPL-X geometry by learning its displacement. Specifically, we freeze the SMPL-X model but improve M_{init} to evolvable \hat{M}_{init} by adding learnable vertex-wise offsets and periodically fit \hat{M}_{init} to the current generated body DMTet at every δ iter-

ation, allowing the learned offsets to model complex body features. The fitting objective is as follows:

$$\mathcal{L}_{\text{fit}} = \lambda_{\text{chamf}} \mathcal{L}_{\text{chamf}} + \lambda_{\text{edge}} \mathcal{L}_{\text{edge}} + \lambda_{\text{nor}} \mathcal{L}_{\text{nor}} + \lambda_{\text{lap}} \mathcal{L}_{\text{lap}}, \quad (5)$$

where $\mathcal{L}_{\text{chamf}}$ is the Chamfer distance between \hat{M}_{init} and the current body geometry, $\mathcal{L}_{\text{edge}}$, \mathcal{L}_{nor} and \mathcal{L}_{lap} are the edge length regularization, normal consistency loss, and Laplacian smoothness, respectively. Through this SMPLX-evolving process, \hat{M}_{init} gradually captures rich geometric features (e.g. muscle contours), providing reliable yet diverse priors for subsequent geometry generation. In addition, unlike SeeAvatar, it maintains the semantics and topology of the SMPL-X model, supporting the subsequent outfit initialization, composition, editing, and animation.

In summary, the loss function for optimizing the human body geometry is as follows:

$$\mathcal{L}_{\text{hum-geo}} = \mathcal{L}_{SDS}^{hn} + \mathcal{L}_{SDS}^{hd} + \lambda_{\text{prior}} \mathcal{L}_{\text{prior}}. \quad (6)$$

Human Body Texture Modeling. Given the human mesh generated from the previous stage, we fix it and utilize a texture field ψ_h which maps a query position to its color to generate a normal-aligned body appearance. Specifically, we employ a MLP network with multi-resolution hash encoding [53] to construct this field and optimize it using ϕ_{hc} with loss as:

$$\nabla_{\psi_h} \mathcal{L}_{SDS}^{hc} = \mathbb{E}_{t,\epsilon} \left[(\epsilon_{\phi_{hc}}(c_t^h; n^h, y_h, t) - \epsilon) \frac{\partial c^h}{\partial \psi_h} \right], \quad (7)$$

where c^h represents the rendered color image of the generated human body. It's worth mentioning that experiments using Physically Based Rendering (PBR) lead to unnatural or unrealistic appearances. Empirically, we adopt simple RGB rendering, and the experimental comparisons are available in the Supp. Mat.

3.4. Apparel Generation

Apparel Initialization. With the body topology retained by our proposed SMPLX-evolving prior loss, we can easily provide semantically aligned initialization for various apparel. Specifically, we utilize the human body segments of SMPL-X and pre-defined masked templates to cover more than a dozen types of daily clothing and accessories. By cropping the corresponding sub-mesh according to the apparel type, we obtain a closed template mesh M_{temp} to initialize the apparel DM Tet through geometry processing such as scaling and sewing. For further details, please refer to the Supp. Mat.

Apparel Geometry Modeling. Similar to human body geometry generation, we utilize human-specific diffusion models to optimize outfits geometry with the SDS loss:

$$\nabla_{\theta_a} \mathcal{L}_{SDS}^{\text{hn}} = \mathbb{E}_{t,\epsilon} \left[(\epsilon_{\phi_{\text{hn}}}(n_t^{\text{a+h}}; y_{\text{a+h}}, t) - \epsilon) \frac{\partial n^{\text{a+h}}}{\partial \theta_a} \right], \quad (8)$$

$$\nabla_{\theta_a} \mathcal{L}_{SDS}^{\text{hd}} = \mathbb{E}_{t,\epsilon} \left[(\epsilon_{\phi_{\text{hd}}}(d_t^{\text{a+h}}; y_{\text{a+h}}, t) - \epsilon) \frac{\partial d^{\text{a+h}}}{\partial \theta_a} \right], \quad (9)$$

where θ_a is the apparel DM Tet parameters, $y_{\text{a+h}}$ is the text description of the appareled avatar, and $n^{\text{a+h}}$ and $d^{\text{a+h}}$ are the rendered appareled human normal and depth maps, respectively. However, human-specific diffusion models are not well-suited for creating clothes and accessories, as they lack of in-domain details and diversity of generated outfits (Sec. 4.4). Hence, we also introduce the object-specific diffusion models proposed by RichDreamer [59], which are trained on large-scale LAION dataset [67].

Concretely, these diffusion models include a normal-depth diffusion model ϕ_{ond} for optimizing the apparel geometry, and a depth-conditional diffusion model ϕ_{oc} for creating the apparel texture. The normal-depth model provides effective supervision for outfit geometry generation by accurately modeling the joint distribution of normal and depth maps using the following SDS loss:

$$\begin{aligned} \nabla_{\theta_a} \mathcal{L}_{SDS}^{\text{ond}} &= \mathbb{E}_{t,\epsilon} \left[(\epsilon_{\phi_{\text{ond}}}(n_t^{\text{a}}; y_{\text{a}}, t) - \epsilon) \frac{\partial n^{\text{a}}}{\partial \theta_a} \right] \\ &+ \mathbb{E}_{t,\epsilon} \left[(\epsilon_{\phi_{\text{ond}}}(d_t^{\text{a}}; y_{\text{a}}, t) - \epsilon) \frac{\partial d^{\text{a}}}{\partial \theta_a} \right], \end{aligned} \quad (10)$$

$$\nabla_{\theta_a} \mathcal{L}_{SDS}^{\text{sdn}} = \mathbb{E}_{t,\epsilon} \left[(\epsilon_{\phi_{\text{sd}}}(n_t^{\text{a}}; y_{\text{a}}, t) - \epsilon) \frac{\partial n^{\text{a}}}{\partial \theta_a} \right], \quad (11)$$

where y_{a} is the text description of a single garment or accessory, and n^{a} and d^{a} are the rendered normal and depth maps of the apparel in the undressed state. Besides, $\mathcal{L}_{SDS}^{\text{sdn}}$ is the vanilla Stable Diffusion (SD) SDS loss enforced on the rendered apparel normal maps. As shown in RichDreamer, native SD helps object-specific diffusion models produce more stable results. In this way, the object-specific diffusion models provide a powerful geometry prior to generating high-fidelity clothes and accessories.

Template-Preserving Loss. Similar to human-specific diffusion models, relying on the object-specific diffusion models may lead to geometric artifacts (*e.g.*, holes, see Sec. 4.4). To address this problem, we propose a template-preserving loss that enforces the apparel geometry to cover the template mesh M_{temp} during the optimization process to ensure geometric integrity. This loss is formulated as follows:

$$\mathcal{L}_{\text{temp}} = \sum_{p \in P_{\text{temp}}} \max(0, s_{\theta_a}(p)), \quad (12)$$

where s_{θ_a} represents the SDF function of apparel DM Tet and P_{temp} is the set of randomly sampled points inside the template mesh.

Specifically, this loss guarantees that the apparel geometry covers the template mesh by pushing the sampled SDF values of s_{θ_a} inside the template mesh to be negative. Instead of employing the MSE function to provide prior constraints such as Eq. (4), the template-preserving loss only restricts the SDF values of the points inside the template, ensuring geometric rationality without limiting the sculpting of geometric details outside the template mesh.

In summary, the loss function for optimizing the apparel geometry is as follows:

$$\mathcal{L}_{\text{app-geo}} = \mathcal{L}_{SDS}^{\text{hn}} + \mathcal{L}_{SDS}^{\text{hd}} + \mathcal{L}_{SDS}^{\text{ond}} + \mathcal{L}_{SDS}^{\text{sdn}} + \lambda_{\text{temp}} \mathcal{L}_{\text{temp}}. \quad (13)$$

Apparel Texture Modeling. Given the generated dress geometry and the textured human body, we employ an object-specific depth-conditional diffusion model for lifelike apparel textures with the following SDS loss:

$$\nabla_{\psi_a} \mathcal{L}_{SDS}^{\text{oc}} = \mathbb{E}_{t,\epsilon} \left[(\epsilon_{\phi_{\text{oc}}}(c_t^{\text{a}}; d^{\text{a}}, y_{\text{a}}, t) - \epsilon) \frac{\partial c^{\text{a}}}{\partial \psi_a} \right], \quad (14)$$

$$\nabla_{\psi_a} \mathcal{L}_{SDS}^{\text{sdc}} = \mathbb{E}_{t,\epsilon} \left[(\epsilon_{\phi_{\text{sd}}}(c_t^{\text{a}}; y_{\text{a}}, t) - \epsilon) \frac{\partial c^{\text{a}}}{\partial \psi_a} \right], \quad (15)$$

where ψ_a and c^{a} is apparel texture field and color image, respectively. Additionally, human-specific diffusion models are combined to optimize the appearance of outfits in the dressed state to ensure basic texture harmony, and the SDS loss is formulated as:

$$\nabla_{\psi_a} \mathcal{L}_{SDS}^{\text{hc}} = \mathbb{E}_{t,\epsilon} \left[(\epsilon_{\phi_{\text{hc}}}(c_t^{\text{a+h}}; n^{\text{a+h}}, y_{\text{a+h}}, t) - \epsilon) \frac{\partial c^{\text{a+h}}}{\partial \psi_a} \right]. \quad (16)$$

In summary, the loss function for optimizing the apparel appearance is as follows:

$$\mathcal{L}_{\text{app-tex}} = \mathcal{L}_{SDS}^{\text{hc}} + \mathcal{L}_{SDS}^{\text{oc}} + \mathcal{L}_{SDS}^{\text{sdc}}. \quad (17)$$

3.5. Unified Texture Refinement

With the stage of human body and apparel generation, we produce human bodies, garments, and accessories with delicate geometry and plausible textures. However, the large domain gap between the training data used to fine-tune different expert models leads to texture incongruity between



Figure 4. Diverse Range of **Barbie-Style** Avatar Generation. Rendering color images and normal images for visualization. **Please zoom in to see the details and see Supp. Mat. for video results.**

the human body and outfits, which significantly impacts the overall realism of the generated digital human (Sec. 4.4).

To address this challenge, we propose a unified texture refinement (UTR) strategy, which jointly fine-tunes the appearance of the assembled avatar under the following multi-step SDS (MSDS):

$$\nabla_{\psi_A} \mathcal{L}_{MSDS}^{hc} = \mathbb{E}_{t, \epsilon} \left[\left(H(c_t^{A+h}; n^{A+h}, y_{A+h}, t) - \epsilon \right) \frac{\partial c^{A+h}}{\partial \psi_A} \right], \quad (18)$$

where $H(\cdot)$ denotes the multi-step operation function (see HumanNorm for more details), $\psi_A = \{\psi_{a_i}, i \in [1, \dots, N]\}$ refers to the parameters of all apparel texture fields, y_{A+h} is the full text description of the avatar wearing all outfits, and n^{A+h} and c^{A+h} are the rendered normal and color images of the avatar wearing all clothes and accessories. Unlike Eq. (17), we only use the human-specific normal-conditioned diffusion model to ensure overall texture style unity. Besides, as the vanilla SDS loss suffers from color oversaturation, we use the MSDS loss to further enhance texture realism, leading to more natural textures. In this way, UTR enhances the texture harmony and consistency of the generated avatar.

3.6. Implementation Details

Our algorithm is implemented using PyTorch [56] and ThreeStudio [18]. Given a text describing an appareled human, e.g., “A man wearing X1 and X2”, we first generate a base human body based on “A man in his underwear”. We then generate the apparel X1 based on “A piece of X1” and “A man wearing X1”, and then generate the apparel X2 based on “A piece of X2” and “A man wearing X1 and X2”. Finally, fine-tune the overall texture based on the full input text “A man wearing X1 and X2”. Additional details can be found in Supp. Mat.

4. Experiments

Some examples of 3D body, garments, and accessories generated by Barbie are shown in Fig. 4. Due to space limitations, only the key experimental settings and results are presented here. For complete results and details, please refer to our Supp. Mat.

4.1. Experimental Settings

Baselines. We quantitatively and qualitatively compare Barbie with the state-of-the-art (SOTA) methods for dressed avatar generation and apparel generation. The compared text-to-avatar methods include DreamWaltz [27], TADA [42], X-Oscar [49], HumanGaussian [44], and HumanNorm [26]. The compared text-to-object methods include DreamFusion [58], Fantasia3D [4], MVDream [69], GaussianDreamer [77], and RichDreamer [59]. Additionally, we conduct a qualitative comparison with recent text-to-disentangled-avatar works [14, 16, 72], though these have not yet released their complete code.

Dataset Construction. We utilized ChatGPT [55] to randomly generate 30 text descriptions of appareled avatars, with each example wearing a top, a bottom, a pair of shoes, and two random accessories. 30 descriptions for dressed humans are used to evaluate avatar generation, and 30×5 apparel descriptions are used to evaluate apparel generation (see the Supp. Mat. for the complete descriptions).

Evaluation Metrics. Existing text-to-3D approaches utilize CLIP-based metrics to evaluate text-image alignment and compare the quality of generated results. However, CLIP-based metrics have been shown [24, 47] to be insufficient to accurately measure the fine-grained correspondence between 3D content and input prompts, which is further confirmed by experiments in the Supp. Mat.

Consequently, inspired by Progressive3D [6], we adopt

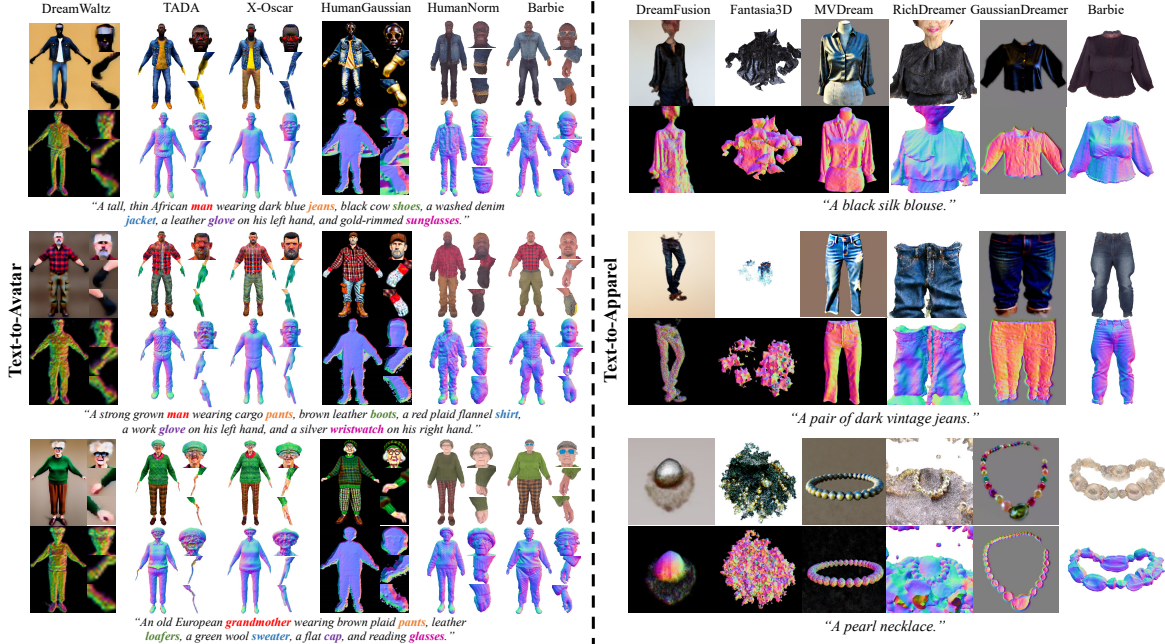


Figure 5. Qualitative comparisons with the SOTA text-to-avatar and text-to-3D methods.

Method	BLIP-VQA \uparrow	BLIP2-VQA \uparrow	GQP \uparrow	TAP \uparrow
DreamWaltz	0.5819	<u>0.5333</u>	5.67	<u>6.67</u>
TADA	0.5306	<u>0.5333</u>	6.33	<u>6.67</u>
X-Oscar	0.5069	0.5292	7.33	2.67
HumanGaussian	<u>0.6222</u>	0.5069	7.00	4.67
HumanNorm	0.5611	0.5292	<u>7.67</u>	<u>6.67</u>
Barbie (Ours)	0.7514	0.5778	66.00	72.67
DreamFusion	0.6633	0.5367	3.33	3.00
Fantasia3D	0.6750	0.4633	0.33	0.33
MVDream	0.7000	0.5933	<u>17.33</u>	<u>15.67</u>
GaussianDreamer	0.7017	0.5283	8.33	11.67
RichDreamer	0.8100	<u>0.6667</u>	6.33	7.33
Barbie (Ours)	<u>0.7917</u>	0.6933	64.33	62.00

Table 1. Quantitative comparisons with the SOTA methods. The best and second-best results are highlighted in **bolded** and underlined, respectively. GQP: generation quality preference (%), TAP: text-image alignment preference (%).

fine-grained text-to-image evaluation metrics including BLIP-VQA [35, 36] and BLIP2-VQA [35, 37] to evaluate the generation capacity of current methods and Barbie. Specifically, we first convert the prompt into multiple separate questions to retrieve corresponding content, then feed the rendered image of the generated content into the VQA model and ask questions one by one, and finally use the probability of answering “yes” as the evaluation metric. For instance, the input avatar prompt “A man wearing X1.” is converted into “Is the person in the picture a man?” and “Is the person in the picture wearing X1?”. The input apparel prompt “A pair of X1.” is converted into “Is the object in the picture a pair of X1?”. Besides, we randomly select 10 examples from the generated results to conduct a user study and ask 30 volunteers to assess (1) generation quality and (2) text-image alignment, and select the preferred methods.

4.2. Comparisons of Dressed Avatar Generation

Comparison with Text-to-Avatar Methods. As shown in the upper part of Tab. 1, our method significantly outperforms the comparison methods across all metrics. The qualitative comparisons illustrated in the left part of Fig. 5 further highlight the strength of our approach. Compared to other methods, the digital humans generated by Barbie exhibit finer and plausible geometric details, and ensure higher alignment with the input text without omitting any clothing or accessories. Additionally, unlike other compared methods, Barbie’s generation process is flexible and controllable, and the generated bodies, clothes, and accessories can be freely combined.

Comparison with Text-to-Decoupled-Avatar Methods. As shown in Fig. 6, our method surpasses TELA [14], LAGA [16], and SO-SMPL [72] in generating refined geometry and lifelike textures. Additionally, Barbie can generate various accessories, including necklaces, glasses, hats, and watches, which are not supported by these methods.

4.3. Comparisons of Apparel Generation

As shown in the lower part of Tab. 1, our approach outperforms other methods on most evaluation metrics and is only slightly lower than RichDreamer (the SOTA open-source text-to-3D method) on BLIP-VQA, ranking the second. The qualitative comparisons illustrated in the right part of Fig. 5 visualize some generation results. Compared to other methods, the clothes and accessories generated by Barbie exhibit more high-fidelity geometry and textures while maintaining high alignment with the text without incorporating incorrect content, such as parts of the human body.

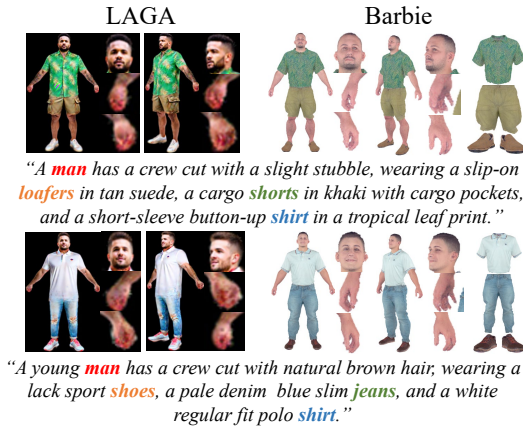


Figure 6. Qualitative comparisons with the text-to-disentangled-avatar work has not yet released the complete code, and their results are copied from their papers. These methods cannot generate diverse accessories shown in Fig. 4 like our Barbie.

4.4. Ablation Study

Effect of SMPLX-Evolving Prior Loss. As shown in Fig. 7-(a), omitting $\mathcal{L}_{\text{prior}}$ results in exaggerated human proportions, greatly reducing the realism of the generated results. Non-evolving human prior loss ensures the rationality of the generated human body, but it leads to over-smooth geometry or limited details. Using the full $\mathcal{L}_{\text{prior}}$ achieves both detailed and reasonable human body geometry generation.

Effect of Template-Preserving Loss. As shown in Fig. 7-(b), the template-preserving loss is crucial to ensure the integrity of dress geometry. Omitting $\mathcal{L}_{\text{temp}}$ can result in holes or other geometry artifacts, significantly reducing the quality of the generated apparel.

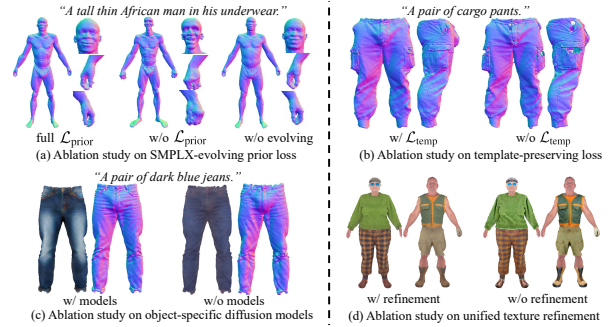


Figure 7. Ablation study on (a) SMPLX-evolving prior loss, (b) template-preserving loss, (c) object-specific diffusion models supervision, and (d) unified texture refinement.

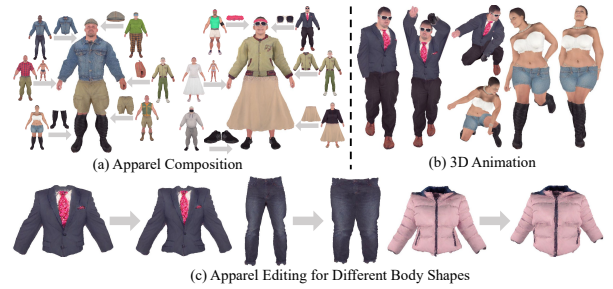


Figure 8. Applications of Barbie.

Effect of Object-Specific Diffusion Models. Fig. 7-(c) shows that introducing an object-specific diffusion model provides powerful guidance for creating finer geometric details and a more lifelike appearance.

Effect of Unified Texture Refinement. Fig. 7-(d) demonstrates that UTR alleviates texture conflict between the human body and outfits. In addition, we also use the VQA model for quantitative comparison. Specifically, BLIP and BLIP2 have 98.33% and 96.67% probability of considering that the results after UTR have a more harmonious texture, which further proves that UTR greatly enhances the realism and consistency of the overall appearance.

4.5. Applications

As shown in Fig. 8-(a), Barbie’s fine-grained decoupling enables the free combination of any human body, garments and accessories, just like dressing Barbie dolls, which greatly improves the playability and reusability of text-to-avatar. With the SMPLX-evolving prior loss, we can obtain an accurate correspondence between the generated human body and the SMPL-X model, which allows us not only to animate the generated avatars utilizing the LBS algorithm as in Fig. 8-(b), but also to easily edit garments for different body shapes as in Fig. 8-(c).

5. Conclusion

We propose Barbie, a novel framework for creating Barbie-style 3D avatars which are dressed in disentangled, detailed, and diverse garments/accessories based on prompts. To

guarantee the domain-specific fidelity of the generated human body and outfits, we suitably combine different specific expert T2I models for domain-specific knowledge. To address the negative impacts caused by the over-strong generative priors of the expert models, we propose a series of well-designed loss functions and optimization strategies to ensure geometric rationality and texture harmony of the generated results. Extensive experiments demonstrate that our approach not only outperforms SOTA methods in both dressed avatar and apparel generation tasks, but also facilitates seamless composition and editing of outfits.

References

- [1] Thimeo Alldieck, Hongyi Xu, and Cristian Sminchisescu. imghum: Implicit generative models of 3d human shape and articulated pose. In *Int. Conf. Comput. Vis.*, pages 5461–5470, 2021. 2
- [2] Bharat Lal Bhatnagar, Garvita Tiwari, Christian Theobalt, and Gerard Pons-Moll. Multi-garment net: Learning to dress 3d people from images. In *Int. Conf. Comput. Vis.*, pages 5420–5430, 2019.
- [3] Yukang Cao, Yan-Pei Cao, Kai Han, Ying Shan, and Kwan-Yee K Wong. Dreamavatar: Text-and-shape guided 3d human avatar generation via diffusion models. In *IEEE Conf. Comput. Vis. Pattern Recog.*, pages 958–968, 2024. 2
- [4] Rui Chen, Yongwei Chen, Ningxin Jiao, and Kui Jia. Fantasia3d: Disentangling geometry and appearance for high-quality text-to-3d content creation. In *Int. Conf. Comput. Vis.*, pages 22246–22256, 2023. 2, 6
- [5] Xu Chen, Tianjian Jiang, Jie Song, Jinlong Yang, Michael J Black, Andreas Geiger, and Otmar Hilliges. gdn: Towards generative detailed neural avatars. In *IEEE Conf. Comput. Vis. Pattern Recog.*, pages 20427–20437, 2022. 1
- [6] Xinhua Cheng, Tianyu Yang, Jianan Wang, Yu Li, Lei Zhang, Jian Zhang, and Li Yuan. Progressive3d: Progressively local editing for text-to-3d content creation with complex semantic prompts. In *Int. Conf. Learn. Represent.*, 2023. 6
- [7] Mehdi Cherti, Romain Beaumont, Ross Wightman, Mitchell Wortsman, Gabriel Ilharco, Cade Gordon, Christoph Schuhmann, Ludwig Schmidt, and Jenia Jitsev. Reproducible scaling laws for contrastive language-image learning. In *IEEE Conf. Comput. Vis. Pattern Recog.*, pages 2818–2829, 2023.
- [8] Patrick John Chia, Giuseppe Attanasio, Federico Bianchi, Silvia Terragni, Ana Rita Magalhães, Diogo Goncalves, Ciro Greco, and Jacopo Tagliabue. Contrastive language and vision learning of general fashion concepts. *Scientific Reports*, 12(1):18958, 2022.
- [9] William J. Clancey. *Transfer of Rule-Based Expertise through a Tutorial Dialogue*. Ph.D. diss., Dept. of Computer Science, Stanford Univ., Stanford, Calif., 1979.
- [10] William J. Clancey. Communication, Simulation, and Intelligent Agents: Implications of Personal Intelligent Machines for Medical Education. In *Proceedings of the Eighth International Joint Conference on Artificial Intelligence (IJCAI-83)*, pages 556–560, Menlo Park, Calif, 1983. IJCAI Organization.
- [11] William J. Clancey. Classification Problem Solving. In *Proceedings of the Fourth National Conference on Artificial Intelligence*, pages 45–54, Menlo Park, Calif., 1984. AAAI Press.
- [12] William J. Clancey. The Engineering of Qualitative Models. Forthcoming, 2021.
- [13] Enric Corona, Albert Pumarola, Guillem Alenya, Gerard Pons-Moll, and Francesc Moreno-Noguer. Smplicit: Topology-aware generative model for clothed people. In *IEEE Conf. Comput. Vis. Pattern Recog.*, pages 11875–11885, 2021.
- [14] Junting Dong, Qi Fang, Zehuan Huang, Xudong Xu, Jingbo Wang, Sida Peng, and Bo Dai. Tela: Text to layer-wise 3d clothed human generation. *arXiv preprint arXiv:2404.16748*, 2024. 2, 3, 6, 7
- [15] Robert Englemore and Anthony Morgan, editors. *Blackboard Systems*. Addison-Wesley, Reading, Mass., 1986.
- [16] Jia Gong, Shenyu Ji, Lin Geng Foo, Kang Chen, Hossein Rahmani, and Jun Liu. Laga: Layered 3d avatar generation and customization via gaussian splatting. *arXiv preprint arXiv:2405.12663*, 2024. 3, 6, 7
- [17] Shuai Guo, Qiuwen Wang, Yijie Gao, Rong Xie, and Li Song. Depth-guided robust and fast point cloud fusion nerf for sparse input views. In *AAAI*, pages 1976–1984, 2024.
- [18] Yuan-Chen Guo, Ying-Tian Liu, Ruizhi Shao, Christian Laforte, Vikram Voleti, Guan Luo, Chia-Hao Chen, Zi-Xin Zou, Chen Wang, Yan-Pei Cao, and Song-Hai Zhang. threestudio: A unified framework for 3d content generation. <https://github.com/threestudio-project/threestudio>, 2023. 6
- [19] Marc Habermann, Weipeng Xu, Michael Zollhoefer, Gerard Pons-Moll, and Christian Theobalt. Livecap: Real-time human performance capture from monocular video. *ACM Trans. Graph.*, 38(2):1–17, 2019.
- [20] Marc Habermann, Weipeng Xu, Michael Zollhofer, Gerard Pons-Moll, and Christian Theobalt. Deepcap: Monocular human performance capture using weak supervision. In *IEEE Conf. Comput. Vis. Pattern Recog.*, pages 5052–5063, 2020.
- [21] Diane Warner Hasling, William J. Clancey, Glenn R. Rennels, and Thomas Test. Strategic Explanations in Consultation—Duplicate. *The International Journal of Man-Machine Studies*, 20(1):3–19, 1983.
- [22] Diane Warner Hasling, William J. Clancey, and Glenn Rennels. Strategic explanations for a diagnostic consultation system. *International Journal of Man-Machine Studies*, 20(1): 3–19, 1984.
- [23] Fangzhou Hong, Mingyuan Zhang, Liang Pan, Zhongang Cai, Lei Yang, and Ziwei Liu. Avatarclip: zero-shot text-driven generation and animation of 3d avatars. *ACM Trans. Graph.*, 41(4):1–19, 2022. 2
- [24] Kaiyi Huang, Kaiyue Sun, Enze Xie, Zhenguo Li, and Xi-hui Liu. T2i-compbench: A comprehensive benchmark for open-world compositional text-to-image generation. In *Adv. Neural Inform. Process. Syst.*, pages 78723–78747, 2023. 6

- [25] Shuo Huang, Zongxin Yang, Liangting Li, Yi Yang, and Jia Jia. Avatarfusion: Zero-shot generation of clothing-decoupled 3d avatars using 2d diffusion. In *ACM Int. Conf. Multimedia*, pages 5734–5745, 2023. 2, 3
- [26] Xin Huang, Ruizhi Shao, Qi Zhang, Hongwen Zhang, Ying Feng, Yebin Liu, and Qing Wang. Humannorm: Learning normal diffusion model for high-quality and realistic 3d human generation. In *IEEE Conf. Comput. Vis. Pattern Recog.*, pages 4568–4577, 2024. 3, 6
- [27] Yukun Huang, Jianan Wang, Ailing Zeng, He Cao, Xianbiao Qi, Yukai Shi, Zheng-Jun Zha, and Lei Zhang. Dreamwaltz: Make a scene with complex 3d animatable avatars. In *Adv. Neural Inform. Process. Syst.*, 2024. 2, 6
- [28] Ajay Jain, Ben Mildenhall, Jonathan T Barron, Pieter Abbeel, and Ben Poole. Zero-shot text-guided object generation with dream fields. In *IEEE Conf. Comput. Vis. Pattern Recog.*, pages 867–876, 2022. 2
- [29] Ruixiang Jiang, Can Wang, Jingbo Zhang, Menglei Chai, Mingming He, Dongdong Chen, and Jing Liao. Avatarcraft: Transforming text into neural human avatars with parameterized shape and pose control. In *Int. Conf. Comput. Vis.*, pages 14371–14382, 2023. 2
- [30] Hanbyul Joo, Tomas Simon, and Yaser Sheikh. Total capture: A 3d deformation model for tracking faces, hands, and bodies. In *IEEE Conf. Comput. Vis. Pattern Recog.*, pages 8320–8329, 2018.
- [31] Bernhard Kerbl, Georgios Kopanas, Thomas Leimkühler, and George Drettakis. 3d gaussian splatting for real-time radiance field rendering. *ACM Trans. Graph.*, 42(4):1–14, 2023. 3
- [32] Nikos Kolotouros, Thiemo Alldieck, Andrei Zanfir, Eduard Bazavan, Mihai Fieraru, and Cristian Sminchisescu. Dreamhuman: Animatable 3d avatars from text. In *Adv. Neural Inform. Process. Syst.*, 2024. 2
- [33] Samuli Laine, Janne Hellsten, Tero Karras, Yeongho Seol, Jaakko Lehtinen, and Timo Aila. Modular primitives for high-performance differentiable rendering. *ACM Trans. Graph.*, 39(6):1–14, 2020. 3
- [34] Boqian Li, Xuan Li, Ying Jiang, Tianyi Xie, Feng Gao, Huamin Wang, Yin Yang, and Chenfanfu Jiang. Garmentdreamer: 3dgs guided garment synthesis with diverse geometry and texture details. *arXiv preprint arXiv:2405.12420*, 2024.
- [35] Dongxu Li, Junnan Li, Hung Le, Guangsen Wang, Silvio Savarese, and Steven C.H. Hoi. LAVIS: A one-stop library for language-vision intelligence. In *Proceedings of the 61st Annual Meeting of the Association for Computational Linguistics (Volume 3: System Demonstrations)*, pages 31–41, 2023. 7
- [36] Junnan Li, Dongxu Li, Caiming Xiong, and Steven Hoi. Blip: Bootstrapping language-image pre-training for unified vision-language understanding and generation. In *International Conference on Machine Learning*, pages 12888–12900, 2022. 7
- [37] Junnan Li, Dongxu Li, Silvio Savarese, and Steven Hoi. Blip-2: Bootstrapping language-image pre-training with frozen image encoders and large language models. In *International Conference on Machine Learning*, pages 19730–19742, 2023. 7
- [38] Kailin Li, Lixin Yang, Zenan Lin, Jian Xu, Xinyu Zhan, Yifei Zhao, Pengxiang Zhu, Wenxiong Kang, Kejian Wu, and Cewu Lu. Favor: Full-body ar-driven virtual object rearrangement guided by instruction text. In *AAAI*, pages 3136–3144, 2024.
- [39] Ruilong Li, Yuliang Xiu, Shunsuke Saito, Zeng Huang, Kyle Olszewski, and Hao Li. Monocular real-time volumetric performance capture. In *Eur. Conf. Comput. Vis.*, pages 49–67, 2020.
- [40] Weiyu Li, Rui Chen, Xuelin Chen, and Ping Tan. Sweetdreamer: Aligning geometric priors in 2d diffusion for consistent text-to-3d. In *Int. Conf. Learn. Represent.*, 2023. 2
- [41] Yixun Liang, Xin Yang, Jiantao Lin, Haodong Li, Xiaogang Xu, and Yingcong Chen. Luciddreamer: Towards high-fidelity text-to-3d generation via interval score matching. In *IEEE Conf. Comput. Vis. Pattern Recog.*, pages 6517–6526, 2024. 2
- [42] Tingting Liao, Hongwei Yi, Yuliang Xiu, Jiayang Tang, Yangyi Huang, Justus Thies, and Michael J. Black. Tada! text to animatable digital avatars. In *International Conference on 3D Vision*, 2024. 2, 3, 6
- [43] Chen-Hsuan Lin, Jun Gao, Luming Tang, Towaki Takikawa, Xiaohui Zeng, Xun Huang, Karsten Kreis, Sanja Fidler, Ming-Yu Liu, and Tsung-Yi Lin. Magic3d: High-resolution text-to-3d content creation. In *IEEE Conf. Comput. Vis. Pattern Recog.*, pages 300–309, 2023. 2
- [44] Xian Liu, Xiaohang Zhan, Jiayang Tang, Ying Shan, Gang Zeng, Dahua Lin, Xihui Liu, and Ziwei Liu. Humangaussian: Text-driven 3d human generation with gaussian splatting. In *IEEE Conf. Comput. Vis. Pattern Recog.*, pages 6646–6657, 2024. 3, 6
- [45] Yufei Liu, Junshu Tang, Chu Zheng, Shijie Zhang, Jinkun Hao, Junwei Zhu, and Dongjin Huang. Clothedreamer: Text-guided garment generation with 3d gaussians. *arXiv preprint arXiv:2406.16815*, 2024.
- [46] Matthew Loper, Naureen Mahmood, Javier Romero, Gerard Pons-Moll, and Michael J Black. Smpl: a skinned multi-person linear model. *ACM Trans. Graph.*, 34(6):1–16, 2015. 2
- [47] Yujie Lu, Xianjun Yang, Xiujun Li, Xin Eric Wang, and William Yang Wang. Llmscore: Unveiling the power of large language models in text-to-image synthesis evaluation. In *Adv. Neural Inform. Process. Syst.*, 2024. 6
- [48] Qianli Ma, Jinlong Yang, Anurag Ranjan, Sergi Pujades, Gerard Pons-Moll, Siyu Tang, and Michael J Black. Learning to dress 3d people in generative clothing. In *IEEE Conf. Comput. Vis. Pattern Recog.*, pages 6469–6478, 2020. 1
- [49] Yiwei Ma, Zhekai Lin, Jiayi Ji, Yijun Fan, Xiaoshuai Sun, and Rongrong Ji. X-oscar: A progressive framework for high-quality text-guided 3d animatable avatar generation. *arXiv preprint arXiv:2405.00954*, 2024. 3, 6
- [50] Mohit Mendiratta, Xingang Pan, Mohamed Elgharib, Kartik Teotia, Ayush Tewari, Vladislav Golyanik, Adam Kortylewski, Christian Theobalt, et al. Avatarstudio: Text-driven editing of 3d dynamic human head avatars. *arXiv preprint arXiv:2306.00547*, 2023. 2

- [51] Ben Mildenhall, Pratul P. Srinivasan, Matthew Tancik, Jonathan T. Barron, Ravi Ramamoorthi, and Ren Ng. Nerf: Representing scenes as neural radiance fields for view synthesis. In *Eur. Conf. Comput. Vis.*, 2020. 3
- [52] Nasir Mohammad Khalid, Tianhao Xie, Eugene Belilovsky, and Tiberiu Popa. Clip-mesh: Generating textured meshes from text using pretrained image-text models. In *ACM SIG-GRAPH Asia*, pages 1–8, 2022. 2
- [53] Thomas Müller, Alex Evans, Christoph Schied, and Alexander Keller. Instant neural graphics primitives with a multi-resolution hash encoding. *ACM Trans. Graph.*, 41(4):1–15, 2022. 3, 4
- [54] NASA. Pluto: The 'other' red planet. <https://www.nasa.gov/nh/pluto-the-other-red-planet>, 2015. Accessed: 2018-12-06.
- [55] OpenAI. Chatgpt. <https://openai.com/>, 2024. 6
- [56] Adam Paszke, Sam Gross, Francisco Massa, Adam Lerer, James Bradbury, Gregory Chanan, Trevor Killeen, Zeming Lin, Natalia Gimelshein, Luca Antiga, et al. Pytorch: An imperative style, high-performance deep learning library. In *Adv. Neural Inform. Process. Syst.*, 2019. 6
- [57] Georgios Pavlakos, Vasileios Choutas, Nima Ghorbani, Timo Bolkart, Ahmed AA Osman, Dimitrios Tzionas, and Michael J Black. Expressive body capture: 3d hands, face, and body from a single image. In *IEEE Conf. Comput. Vis. Pattern Recog.*, pages 10975–10985, 2019. 2, 3
- [58] Ben Poole, Ajay Jain, Jonathan T Barron, and Ben Mildenhall. Dreamfusion: Text-to-3d using 2d diffusion. In *Int. Conf. Learn. Represent.*, 2022. 2, 3, 6
- [59] Lingteng Qiu, Guanying Chen, Xiaodong Gu, Qi Zuo, Mutian Xu, Yushuang Wu, Weihao Yuan, Zilong Dong, Liefeng Bo, and Xiaoguang Han. Richdreamer: A generalizable normal-depth diffusion model for detail richness in text-to-3d. In *IEEE Conf. Comput. Vis. Pattern Recog.*, pages 9914–9925, 2024. 2, 5, 6
- [60] Alec Radford, Jong Wook Kim, Chris Hallacy, Aditya Ramesh, Gabriel Goh, Sandhini Agarwal, Girish Sastry, Amanda Askell, Pamela Mishkin, Jack Clark, et al. Learning transferable visual models from natural language supervision. In *International Conference on Machine Learning*, pages 8748–8763, 2021. 2
- [61] Anurag Ranjan, Timo Bolkart, Soubhik Sanyal, and Michael J Black. Generating 3d faces using convolutional mesh autoencoders. In *Eur. Conf. Comput. Vis.*, pages 704–720, 2018. 1
- [62] James Rice. Poligon: A System for Parallel Problem Solving. Technical Report KSL-86-19, Dept. of Computer Science, Stanford Univ., 1986.
- [63] Arthur L. Robinson. New ways to make microcircuits smaller. *Science*, 208(4447):1019–1022, 1980.
- [64] Arthur L. Robinson. New Ways to Make Microcircuits Smaller—Duplicate Entry. *Science*, 208:1019–1026, 1980.
- [65] Robin Rombach, Andreas Blattmann, Dominik Lorenz, Patrick Esser, and Björn Ommer. High-resolution image synthesis with latent diffusion models. In *IEEE Conf. Comput. Vis. Pattern Recog.*, pages 10684–10695, 2022. 2
- [66] Aditya Sanghi, Hang Chu, Joseph G Lambourne, Ye Wang, Chin-Yi Cheng, Marco Fumero, and Kamal Rahimi Malekshah. Clip-forge: Towards zero-shot text-to-shape generation. In *IEEE Conf. Comput. Vis. Pattern Recog.*, pages 18603–18613, 2022. 2
- [67] Christoph Schuhmann, Romain Beaumont, Richard Vencu, Cade Gordon, Ross Wightman, Mehdi Cherti, Theo Coombes, Aarush Katta, Clayton Mullis, Mitchell Wortsman, et al. Laion-5b: An open large-scale dataset for training next generation image-text models. In *Adv. Neural Inform. Process. Syst.*, pages 25278–25294, 2022. 5
- [68] Tianchang Shen, Jun Gao, Kangxue Yin, Ming-Yu Liu, and Sanja Fidler. Deep marching tetrahedra: a hybrid representation for high-resolution 3d shape synthesis. In *Adv. Neural Inform. Process. Syst.*, pages 6087–6101, 2021. 3
- [69] Yichun Shi, Peng Wang, Jianglong Ye, Long Mai, Kejie Li, and Xiao Yang. Mvdream: Multi-view diffusion for 3d generation. In *Int. Conf. Learn. Represent.*, 2023. 2, 6
- [70] Jiayang Tang, Jiawei Ren, Hang Zhou, Ziwei Liu, and Gang Zeng. Dreamgaussian: Generative gaussian splatting for efficient 3d content creation. In *Int. Conf. Learn. Represent.*, 2023. 2
- [71] Ashish Vaswani, Noam Shazeer, Niki Parmar, Jakob Uszkoreit, Llion Jones, Aidan N. Gomez, Lukasz Kaiser, and Illia Polosukhin. Attention is all you need, 2017.
- [72] Jionghao Wang, Yuan Liu, Zhiyang Dou, Zhengming Yu, Yongqing Liang, Xin Li, Wenping Wang, Rong Xie, and Li Song. Disentangled clothed avatar generation from text descriptions. *arXiv preprint arXiv:2312.05295*, 2023. 2, 3, 6, 7
- [73] Peng Wang, Lingjie Liu, Yuan Liu, Christian Theobalt, Taku Komura, and Wenping Wang. Neus: Learning neural implicit surfaces by volume rendering for multi-view reconstruction. In *Adv. Neural Inform. Process. Syst.*, pages 27171–27183, 2021. 2, 3
- [74] Yi Wang, Jian Ma, Ruizhi Shao, Qiao Feng, Yu-Kun Lai, Yebin Liu, and Kun Li. Humancoser: Layered 3d human generation via semantic-aware diffusion model. *arXiv preprint arXiv:2312.05804*, 2023. 3
- [75] Zhengyi Wang, Cheng Lu, Yikai Wang, Fan Bao, Chongxuan Li, Hang Su, and Jun Zhu. Prolificdreamer: High-fidelity and diverse text-to-3d generation with variational score distillation. In *Adv. Neural Inform. Process. Syst.*, 2024. 2
- [76] Yuanyou Xu, Zongxin Yang, and Yi Yang. Seeavatar: Photorealistic text-to-3d avatar generation with constrained geometry and appearance. *arXiv preprint arXiv:2312.08889*, 2023. 3, 4
- [77] Taoran Yi, Jiemin Fang, Junjie Wang, Guanjun Wu, Lingxi Xie, Xiaopeng Zhang, Wenyu Liu, Qi Tian, and Xinggang Wang. Gaussiandreamer: Fast generation from text to 3d gaussians by bridging 2d and 3d diffusion models. In *IEEE Conf. Comput. Vis. Pattern Recog.*, pages 6796–6807, 2024. 2, 6
- [78] Ye Yuan, Xueting Li, Yangyi Huang, Shalini De Mello, Koki Nagano, Jan Kautz, and Umar Iqbal. Gavatar: Animatable 3d gaussian avatars with implicit mesh learning. In *IEEE Conf. Comput. Vis. Pattern Recog.*, pages 896–905, 2024. 3

- [79] Huichao Zhang, Bowen Chen, Hao Yang, Liao Qu, Xu Wang, Li Chen, Chao Long, Feida Zhu, Daniel Du, and Min Zheng. Avatarverse: High-quality & stable 3d avatar creation from text and pose. In *AAAI*, pages 7124–7132, 2024. [2](#)
- [80] Lvmin Zhang, Anyi Rao, and Maneesh Agrawala. Adding conditional control to text-to-image diffusion models. In *Int. Conf. Comput. Vis.*, pages 3836–3847, 2023. [2](#)
- [81] Yang Zheng, Ruizhi Shao, Yuxiang Zhang, Tao Yu, Zerong Zheng, Qionghai Dai, and Yebin Liu. Deepmulticap: Performance capture of multiple characters using sparse multiview cameras. In *Int. Conf. Comput. Vis.*, pages 6239–6249, 2021.
- [82] Heming Zhu, Yu Cao, Hang Jin, Weikai Chen, Dong Du, Zhangye Wang, Shuguang Cui, and Xiaoguang Han. Deep fashion3d: A dataset and benchmark for 3d garment reconstruction from single images. In *Eur. Conf. Comput. Vis.*, pages 512–530, 2020.
- [83] Luyang Zhu, Konstantinos Rematas, Brian Curless, Steven M Seitz, and Ira Kemelmacher-Shlizerman. Reconstructing nba players. In *Eur. Conf. Comput. Vis.*, pages 177–194, 2020.